# Elemental sulfur-based autotrophic denitrification and denitritation: microbially catalyzed sulfur hydrolysis and nitrogen conversions

**Author names and affiliations:** Anastasiia Kostrytsia[1*], Stefano Papirio[2], Luigi Frunzo[3], Maria Rosaria Mattei[3], Estefanía Porca[4], Gavin Collins[4], Piet N. L. Lens[5], Giovanni Esposito[1]

[1] Department of Civil and Mechanical Engineering, University of Cassino and Southern Lazio, via Di Biasio 43, 03043 Cassino (FR), Italy

[2] Department of Civil, Architectural and Environmental Engineering, University of Naples Federico II, via Claudio 21, 80125 Naples, Italy

[3] Department of Mathematics and Applications "*Renato Caccioppoli*", University of Naples Federico II, via Cintia, Monte S. Angelo, 1-80126 Naples, Italy

[4] Microbial Communities Laboratory, School of Natural Sciences and Ryan Institute, National University of Ireland Galway, University Road, Galway H91 TK33, Ireland

[5] UNESCO-IHE, Institute for Water Education, PO Box 3015, 2601 DA Delft, The Netherlands

[*]**Corresponding author**: Anastasiia Kostrytsia. E-mail address: kostritsia@gmail.com.

**Present address:** Department of Civil and Mechanical Engineering, University of Cassino and Southern Lazio, via Gaetano Di Biasio 43, 03043 Cassino (FR), Italy.

**ABSTRACT**: The hydrolysis of elemental sulfur ($S^0$) coupled to $S^0$-based denitrification and denitritation was investigated in batch bioassays by microbiological and modeling approaches. In the denitrification experiments, the highest obtained $NO_3^-$-N removal rate was 20.9 mg/l·d. In the experiments with the biomass enriched on $NO_2^-$, a $NO_2^-$-N removal rate of 10.7 mg/l·d was achieved even at a $NO_2^-$-N concentration as high as 240 mg/l. The *Helicobacteraceae* family was only observed in the biofilm attached onto the chemically-synthesized $S^0$ particles with a relative abundance up to 37.1%, suggesting it was the hydrolytic biomass capable of $S^0$ solubilization in the novel surface-based model. $S^0$-driven denitrification was modeled as a two-step process in order to explicitly account for the sequential reduction of $NO_3^-$ to $NO_2^-$ and then to $N_2$ by denitrifying bacteria.

**KEYWORDS**: Autotrophic denitrification; autotrophic denitritation; elemental sulfur; community structure; surface-based hydrolysis; mathematical modeling.

## 1. INTRODUCTION

The removal of nitrate ($NO_3^-$) and nitrite ($NO_2^-$) is one of the main concerns in wastewater treatment plants. High-strength $NO_3^-$ wastewaters are produced by petrochemical, metal finishing, fertilizer and nuclear industries (Li et al., 2016). Contamination by $NO_3^-$ results in eutrophication and ecological disturbance of ground and surface water bodies (Sun and Nemati, 2012). Compared to $NO_3^-$, $NO_2^-$ induces a higher toxicity towards aquatic life, including bacteria (Philips et al., 2002). Additionally, elevated $NO_3^-$ and $NO_2^-$ concentrations can lead to human health disorders such as infant methemoglobinemia, non-Hodgkin's lymphoma and intestine cancer (Barrett et al., 2013; Liu et al., 2016).

The conventional processes aimed at $NO_3^-$ and $NO_2^-$ removal are denitrification and denitritation, respectively. Generally, denitrification is performed by heterotrophic bacteria in anoxic environments and in the presence of organic compounds (Papirio et al., 2014; Zou et al. 2015). For the treatment of wastewaters poor in organics, autotrophic denitrification with chemically-synthesized $S^0$ can be used alternatively. The main advantages of autotrophic denitrification and denitritation are: (1) inorganic compounds are used as electron donors, decreasing the risk associated with residual organics; (2) no external organic carbon is required to maintain the process, reducing the operating costs; (3) a lower cell yield results in less sludge production and, thus, lower sludge treatment costs; and (4) less $N_2O$ is generally produced (Zhang et al., 2015b; Zhou et al., 2015).

The limited water solubility of chemically-synthesized $S^0$ remains, however, a major obstacle to full-scale autotrophic denitrification applications (Park and Yoo, 2009). $S^0$ is

solely taken up by denitrifying microorganisms after its solubilization and diffusion into the cells (Moraes and Foresti, 2012). Because of the rather insoluble properties of the $S^0$ particles, a preliminary hydrolysis to make $S^0$ soluble and bioavailable occurs (Wang et al., 2016). Some sulfur-oxidizing bacteria are capable of $S^0$ solubilization to bioavailable polysulfide ($S_n^{2-}$) or thiol-bound sulfane sulfur atoms ($GSS_nH$), which can be further transported into the periplasm and oxidized to $SO_4^{2-}$ (Wang et al., 2016). The bacteria from the genera *Thiobacillus*, *Sulfurimona*s and *Ignavibacteriales* have been found to dominate the consortia in autotrophic denitrification with $S^0$ (Zhang et al., 2015a). However, the bacterial communities involved in the dissolution of $S^0$ as well as $S^0$-driven autotrophic denitrification and denitritation need to be further studied.

Most mathematical models simulating chemolithotrophic denitrification with $S^0$ are single-substrate and one-step denitrification models, which account for direct $NO_3^-$ conversion to dinitrogen gas ($N_2$) linked to $S^0$ oxidation (Batchelor and Lawrence, 1978; Qambrani et al., 2015). However, some studies demonstrated that the production of $NO_2^-$ during the autotrophic denitrification decreases the overall process efficiency (Park and Yoo, 2009). The feed pH, the source of electron donor, the sulfur to nitrogen (S/N) ratio and the microbial community structure affect the extent of the $NO_2^-$ accumulation (Christianson et al., 2015; Du et al., 2016; Guerrero et al., 2016). Besides, also nitrous oxide ($N_2O$) can be produced (Liu et al., 2016). Recently, an autotrophic denitrification kinetic model with $S^0$ as electron donor has been developed (Liu et al., 2016). Nonetheless, none of these studies explicitly modeled the likely rate limiting step, i.e. the solubilization of $S^0$ (Sierra-Alvarez et al., 2007).

The main objective of this research was to investigate the solubilization of chemically-synthesized $S^0$ and the subsequent $S^0$-driven autotrophic denitrification and denitritation in batch bioassays. The composition and performance of the microbial community of both suspended biomass and the biofilm onto the $S^0$ lentils involved in the $S^0$ solubilization during denitrification and denitritation were investigated. Based on the experimental evidence, a model accounting for the microbially catalyzed surface-based $S^0$ solubilization and two-step denitrification is proposed.

## 2. MATERIALS AND METHODS

### 2.1 Enrichment of Biomass

The autotrophic denitrifying biomass used in this study was enriched for 3 months in serum bottles using activated sludge collected from the denitrification basin of the municipal wastewater treatment plant (WWTP) of Cassino (Italy) as inoculum. The concentration of suspended volatile solids (VS) of the activated sludge was 4.2 g/l. The tap water basal medium contained the following components (per l): 0.4 g $NH_4Cl$, 0.3 g $KH_2PO_4$, 0.8 g $K_2HPO_4$, 0.021 g $MgCl_2{\cdot}6H_2O$. Trace elements were supplied from a stock solution (10 ml/l). The trace element solution was prepared by dissolving the following compounds in a solution (per l): 1.5 g nitrilotriacetic acid disodium salt ($C_6H_7NNa_2O_6$), 3.0 g $MgSO_4{\cdot}7H_2O$, 0.5 g $MnSO_4$, 1.0 g NaCl, 0.1 g $FeSO_4{\cdot}7H_2O$, 0.1 g $CaCl_2{\cdot}2H_2O$, 0.1 g $CoCl_2{\cdot}6H_2O$, 0.13 g ZnCl, 0.01 g $CuSO_4{\cdot}5H_2O$, 0.01 g $AlK(SO_4)_2{\cdot}12H_2O$, 0.01 g $H3BO_3$, 0.025 g $Na_2MoO4{\cdot}2H_2O$.

The activated sludge was maintained in suspension and added to each bottle with a 10% (v/v) amount. $NO_3^-$ and $NO_2^-$ were used separately as electron acceptors at a concentration of approximately 225 mg/l as $NO_3^-$-N and $NO_2^-$-N in each bottle. $S^0$ lentils (particles with an average size between 2 and 4 mm and a $S^0$ content of approximately 99%, purchased from a local agricultural supply store) were used as both electron donor and carrier for the growth of the denitrifying biomass. 2.1 g of $S^0$ (corresponding to 54 ± 8 sulfur lentils) was added to each bottle. pH was adjusted to 7.5 by using 1 M NaOH. $CaCO_3$ was added as buffer and carbon source with a $S^0$:$CaCO_3$ (g/g) ratio of 1.5.

Each bottle was purged with helium gas for 3 min to exclude free oxygen and background nitrogen, and then sealed with a rubber stopper and an aluminum crimp. Finally, all the bottles were placed in a water bath at 30 (± 2)°C and on a gyratory shaker at 300 rpm. The enrichment was subcultured every three weeks or as soon as $NO_3^-$-N or $NO_2^-$-N degradation stopped. An enrichment was considered stable when the obtained denitrification or denitritation rates of the subcultures varied by less than 5%.

**2.2 Kinetic Experiments**

Three batch experiments were carried out to study the kinetics of $S^0$-driven autotrophic denitrification ($NO_3^-$and $S^0$), denitritation ($NO_2^-$ and $S^0$) and simultaneous denitrification-denitritation ($NO_2^-$, $NO_3^-$ and $S^0$) coupled to $S^0$ solubilization in 125 ml glass serum bottles with a working volume of 100 ml. **Table 1** reports the operating conditions. The basal medium and trace elements were added to each bottle at the same concentrations as in the enrichment phase. An initial suspended VS concentration of 1.0 g/l was used. $S^0$ lentils were supplied in a concentration of 21 g/l. 14 g/l of $CaCO_3$ was provided according

122 to the $S^0$:$CaCO_3$ (g/g) ratio of 1.5. Controls without biomass were performed to evaluate
123 possible abiotic reactions between $S^0$ and $NO_3^-$ or $NO_2^-$. Additionally, controls without
124 electron donor ($S^0$) or electron acceptor ($NO_3^-$ or $NO_2^-$) were carried out to estimate $NO_3^-$
125 and $NO_2^-$ degradation or $S^0$ oxidation, respectively, not associated with autotrophic
126 denitrification or denitritation. The purging and sealing of the bottles were performed as
127 during the enrichment phase. All the bioassays were performed in triplicate. The serum
128 bottles were placed on a gyratory shaker (300 rpm) at a controlled temperature of 30 (±
129 2)°C.
130
131 **Table 1.** Experimental conditions used in the batch experiments investigating $S^0$-driven denitrification
132 ($NO_3^-$-N and $S^0$), denitritation ($NO_2^-$-N and $S^0$) and simultaneous denitrification-denitritation ($NO_2^-$-N,
133 $NO_3^-$-N and $S^0$) at 30 (± 2)°C and 300 rpm.

| Experiment | Initial concentration (mg/l) | | | | pH |
|---|---|---|---|---|---|
| | $NO_2^-$-N | $NO_3^-$-N | Total N | Suspended VS | |
| Denitrification ($NO_3^-$and $S^0$) | 30 | 210 | 240 | 1000[a] | 7.4±0.1 |
| Denitritation ($NO_2^-$ and $S^0$) | 240 | - | 240 | 1000[b] | 7.4±0.1 |
| Denitritation and denitrification ($NO_2^-$, $NO_3^-$ and $S^0$) | 110 | 60 | 170 | 1000[a] | 7.3±0.1 |
| $NO_3^-$- and $NO_2^-$-free control | - | - | - | 1000[c] | 7.5±0.1 |
| $S^0$-free controls | - | 210 | 210 | 1000[a] | 7.5±0.1 |
| | 240 | - | 240 | 1000[b] | 7.5±0.1 |

| | | | | | |
|---|---|---|---|---|---|
| Abiotic controls | - | 210 | 210 | - | 7.5±0.1 |
| | 240 | - | 240 | - | 7.5±0.1 |

[a] Microbial source: biomass enriched on $NO_3^-$-N and $S^0$, see **Section 2.1**

[b] Microbial source: biomass enriched on $NO_2^-$-N and $S^0$, see **Section 2.1**

[c] Microbial source: raw activated sludge (non-enriched)

### 2.3 Microbial Community Analysis

The total bacterial DNA was extracted in triplicate from both the suspended biomass and biofilm attached onto the $S^0$ particles ($S^0$ lentils) of each batch bioassay at the beginning and the end of the experiments according to the protocol by Griffiths et al. (2000). The extracted DNA was quantified by a UV-Vis spectrophotometer (NanoDrop Technologies, Wilmington, USA) prior to being stored at -20°C for subsequent molecular analysis. Samples of DNA were sent to FISABIO (Valencia, Spain) for high-throughput sequencing of the 16S rRNA gene on an Illumina MiSeq platform. Forward and reverse primers for PCR were 515f and 806r, respectively (Caporaso et al., 2010). A total of 492111 raw sequences were obtained from the samples. Sequence screening, alignment to Silva (v.123) database, clustering, chimeras removal and taxonomic classification were performed using Mothur v1.39.3 (Schloss et al., 2009). Each dataset was subsampled to the lowest read count (n = 31192) and all analyses were based on the final subsampled data sets. A threshold of 1% was employed to define rare or abundant taxa. Raw sequence data were deposited as FASTQ files in the National Center for Biotechnology Information (NCBI) with the accession number SRP126842.

## 2.4 Sampling and Analytical Methods

Samples of the liquid phase were taken with 5-ml disposable syringes and needles to avoid oxygen transfer into the bottles. Sampling was performed once per week during the enrichment phase and twice a day in the batch kinetic experiments. Prior to and at the end of the batch kinetic experiments, 10 ml of the liquid phase was taken for VS determination. Simultaneously, 2 g of mixed solid ($S^0$ lentils and $CaCO_3$ particles) was removed for visualization of biofilm formation on its surface as well as VS analysis. All the liquid samples were filtered with 0.2 µm cellulose membranes (Merck Millipore, USA) and stored at -20°C prior to analysis. $NO_3^-$, $NO_2^-$, $S_2O_3^{2-}$ and $SO_4^{2-}$ concentrations were analyzed by ion chromatography (IC) using a 883 Basic IC Plus (Metrohm, Switzerland) equipped with a 4-mm Metrosep A Supp 5-150 column, a Metrosep A Supp 4/5 guard column and a 863 Compact autosampler. Dissolved oxygen (DO) was measured with a Multi 3410 DO-meter (WTW GmbH, Germany), equipped with a FDO-925 DO sensor. pH and temperature were measured using a Sentix 940-3 probe. VS were measured according to the Standard Methods (APHA, 2011).

Adhering cells on the surface of the mixed solids were visualized by means of scanning electron microscopy (SEM). The fixation of the mixed solids was carried out in 2.5% glutaraldehyde with 0.2 M sodium cacodylate buffer (Sigma-Aldrich, Germany) at 4°C for 16 h. Subsequently, the fixed particles were dehydrated through a graded series of 50-100% ethanol. Finally, the samples were gold-sputter coated and mounted onto stubs and viewed in a S2600N variable pressure scanning electron microscope (Hitachi, Japan).

## 2.5 Model Development and Numerical Approach

A kinetic model simulating $S^0$-based two-step denitrification coupled to $S^0$ dissolution and its further oxidation is proposed. The model considered the activities of two microbial species: the autotrophic denitrifying bacteria using $NO_3^-$ or $NO_2^-$ as electron acceptors and a hydrolytic biomass growing on the $S^0$ lentils. The model evaluated the interactions between the related physical and biochemical processes, $S^0$ solubilization and $S^0$-based denitrification and denitritation (**Figure 1**). $S^0$-driven autotrophic denitrification was modeled as a two-step process: the sequential conversion of $NO_3^-$ to $NO_2^-$ with its further reduction to $N_2$ by denitrifying bacteria was considered (Mattei et al., 2015a). The kinetics of nitric oxide (NO) and nitrous oxide ($N_2O$) formation and reduction were neglected due to time-scale considerations (Sin et al., 2008).

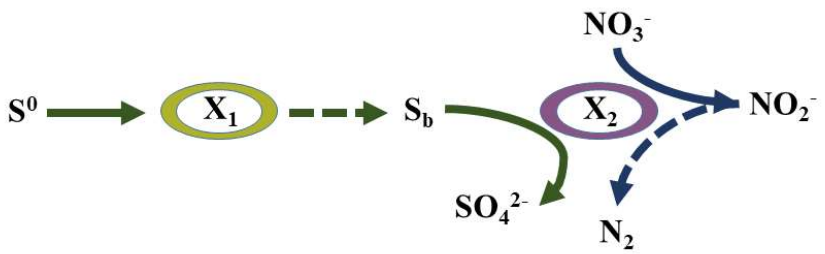


**Figure 1.** Schematic representation of the proposed model for $S^0$ solubilization and two-step denitrification. $S^0$: elemental sulfur, $S_b$: bioavailable sulfur, $NO_3^-$: nitrate, $NO_2^-$: nitrite, $N_2$: dinitrogen gas, $SO_4^{2-}$: sulfate, $X_1$: hydrolytic biomass and $X_2$: denitrifying biomass.

The dissolution of chemically produced $S^0$ is known to be the rate-limiting step for autotrophic denitrification (Liu et al., 2016; Sierra-Alvarez et al., 2007). The specific surface area is the key parameter for the microbial hydrolysis of insoluble compounds

insofar it is related to the number of bacteria attached onto their surface (Esposito et al., 2011a; Vavilin et al., 2008). Therefore, the biological surface-based solubilization of $S^0$ was explicitly modeled prior to its oxidation to $SO_4^{2-}$. $S^0$ uptake was modeled by introducing a new state variable, the bioavailable sulfur ($S_b$), which represents the soluble compound produced by the hydrolytic biomass and eventually taken up by denitrifying bacteria for further oxidation to $SO_4^{2-}$. The model did not account for potential redox processes involved in the $S^0$ solubilization, as the hydrolytic biomass was not considered to remove $NO_3^-$ or $NO_2^-$.

The model equations were derived from mass conservation principles and formulated in terms of two microbial components, namely the hydrolytic $X_1$ and denitrifying $X_2$ biomasses, and six reacting components considered simultaneously: elemental sulfur $S_1$, bioavailable sulfur $S_2$, nitrate $S_3$, nitrite $S_4$, nitrogen gas $S_5$ and sulfate $S_6$. The equations were expressed as follows (or as matrix in **Table S1** in **Supplementary Material**):

$$\frac{dS_1}{dt} = -k_1 \frac{S_1}{\frac{K_1}{a^*}+S_1} X_1, \quad \textbf{(3.1)}$$

$$\frac{dS_2}{dt} = k_1 \frac{S_1}{\frac{K_1}{a^*}+S_1} X_1 - \frac{r_1}{Y_{2,3}} \mu_{2,3}^{max} \frac{S_2}{K_{2,2}+S_2} \frac{(S_3-S_3^*)}{K_{2,3}+(S_3-S_3^*)} \frac{S_3}{S_3+S_4} X_2 - \frac{r_2}{Y_{2,4}} \mu_{2,4}^{max} \frac{S_2}{K_{2,2}+S_2} \frac{(S_4-S_4^*)}{K_{2,4}+(S_4-S_4^*)} \frac{S_4}{S_3+S_4} X_2, \quad \textbf{(3.2)}$$

$$\frac{dS_3}{dt} = -\frac{1}{Y_{2,3}} \mu_{2,3}^{max} \frac{S_2}{K_{2,2}+S_2} \frac{(S_3-S_3^*)}{K_{2,3}+(S_3-S_3^*)} \frac{S_3}{S_3+S_4} X_2, \quad \textbf{(3.3)}$$

$$\frac{dS_4}{dt} = \frac{1}{Y_{2,3}} \mu_{2,3}^{max} \frac{S_2}{K_{2,2}+S_2} \frac{(S_3-S_3^*)}{K_{2,3}+(S_3-S_3^*)} \frac{S_3}{S_3+S_4} X_2 - \frac{1}{Y_{2,4}} \mu_{2,4}^{max} \frac{S_2}{K_{2,2}+S_2} \frac{(S_4-S_4^*)}{K_{2,4}+(S_4-S_4^*)} \frac{S_4}{S_3+S_4} X_2, \quad \textbf{(3.4)}$$

$$\frac{dS_5}{dt} = \frac{1}{Y_{2,4}}\mu_{2,4}^{max}\frac{S_2}{K_{2,2}+S_2}\frac{(S_4-S_4^*)}{K_{2,4}+(S_4-S_4^*)}\frac{S_4}{S_3+S_4}X_2, \quad \textbf{(3.5)}$$

$$\frac{dS_6}{dt} = \frac{r_1}{Y_{2,3}}\mu_{2,3}^{max}\frac{S_2}{K_{2,2}+S_2}\frac{(S_3-S_3^*)}{K_{2,3}+(S_3-S_3^*)}\frac{S_3}{S_3+S_4}X_2 + \frac{r_2}{Y_{2,4}}\mu_{2,4}^{max}\frac{S_2}{K_{2,2}+S_2}\frac{(S_4-S_4^*)}{K_{2,4}+(S_4-S_4^*)}\frac{S_4}{S_3+S_4}X_2, \quad \textbf{(3.6)}$$

$$\frac{dX_1}{dt} = K_0 k_1 \frac{S_1}{\frac{K_1}{a^*}+S_1}X_1 - k_{d,1}X_1, \quad \textbf{(3.7)}$$

$$\frac{dX_2}{dt} = \mu_{2,3}^{max}\frac{S_2}{K_{2,2}+S_2}\frac{(S_3-S_3^*)}{K_{2,3}+(S_3-S_3^*)}\frac{S_3}{S_3+S_4}X_2 + \mu_{2,4}^{max}\frac{S_2}{K_{2,2}+S_2}\frac{(S_4-S_4^*)}{K_{2,4}+(S_4-S_4^*)}\frac{S_4}{S_3+S_4}X_2 - k_{d,2}\cdot X_2 \quad \textbf{(3.8)}$$

where $k_1$ denotes the hydrolysis kinetic constant for $S_1$; $a^*$ represents the mass specific area; $K_1$ the volume specific half-saturation constant for $S_1$; $k_{d,i}$ the decay constant of species $i$; $Y_{i,j}$, $K_{i,j}$ and $\mu_{i,j}^{max}$ denote the yield, the half-saturation constant and the maximum growth rate of species $i$ on substrate $j$, respectively; $K_0$ represents the efficiency growth coefficient for $X_1$; $r_1$ and $r_2$ are the stoichiometric $S_2$ to $S_3$ and $S_2$ to $S_4$ ratios, respectively. The values of $Y_{2,3}$, $Y_{2,4}$, $K_{2,2}$, $K_{2,4}$, $r_1$, $r_2$, $k_{d,1}$ and $k_{d,2}$ were adopted from previous studies (Liu et al., 2016; Sierra-Alvarez et al., 2007; Sin et al., 2008; Xu et al., 2016). The optimal values of $\mu_{2,3}^{max}$ and $\mu_{2,4}^{max}$ were deducted from both the denitrification and denitritation experiments (**Table 2**).

**Table 2.** Stoichiometric and kinetic parameters of the developed model for two-step autotrophic denitrification with $S^0$.

| Parameter | | Value | Unit | Source |
|---|---|---|---|---|
| | **Stoichiometric parameters** | | | |
| $Y_{2,3}$ | Yield coefficient for $X_2$ on $S_3$ | 0.25 | mg VS/mg N | Xu et al., 2016 |

| | | | | |
|---|---|---|---|---|
| $Y_{2,4}$ | Yield coefficient for $X_2$ on $S_4$ | 0.28 | mg VS/mg N | Xu et al., 2016 |
| $r_1$ | $S_2$ to $S_3$ stochiometric ratio | 1.2 | mg S/mg N | Sierra-Alvarez et al., 2007 |
| $r_2$ | $S_2$ to $S_4$ stochiometric ratio | 0.55 | mg S/mg N | Sierra-Alvarez et al., 2007 |
| | **Kinetic parameters** | | | |
| $K_0$ | Efficiency growth coefficient for $X_1$ | 0.1 | mg VS/mg S | This study |
| $\mu_{2,3}^{max}$ | Maximum growth rate for $X_2$ on $S_3$ | 0.0067 | 1/d | This study [d] |
| $\mu_{2,4}^{max}$ | Maximum growth rate for $X_2$ on $S_4$ | 0.0058 | 1/d | This study [d] |
| $K_{2,2}$ | Half-saturation constant for $S_2$ | 0.215 | mg S/l | Liu et al., 2016 |
| $K_{2,3}$ | Half-saturation constant for $S_3$ | 36 | mg N/l | This study [e] |
| $S_3^*$ | The threshold value for $S_3$ | 35 | mg N/l | This study [d] |
| $K_{2,4}$ | Half-saturation constant for $S_4$ | 40 | mg N/l | Xu et al., 2016 |
| $S_4^*$ | The threshold value for $S_4$ | 37 | mg N/l | This study [e] |
| $K_1$ | Volume specific half-saturation constant for $S_1$ | 5.1 | 1/dm | This study |
| $k_1$ | Hydrolysis kinetic constant | 0.12 | mg S/mg VS·d | This study |
| $a^*$ | Mass specific area | 0.0008164 | $dm^2$/mg | Calculated |
| $k_{d,1}$ | Decay rate coefficient for $X_1$ | 0.0006 | 1/d | Sin et al., 2008 |
| $k_{d,2}$ | Decay rate coefficient for $X_2$ | 0.0006 | 1/d | Sin et al., 2008 |

[d] Denitrification experiments

[e] Denitritation experiments

Eq. (**3.1**) governs the dynamics of $S_1$ solubilization and is newly formulated as a modified surface-based kinetic equation to account for the hydrolysis of $S_1$ by $X_1$ (Esposito et al., 2011b; Hills and Nakano, 1984). The concentration and specific surface area of the

**Commentato [SP1]:** stoichiometric

**Commentato [SP2]:** stoichiometric

substrate to be hydrolyzed ($S_1$) as well as the concentration of the hydrolytic biomass ($X_1$) are identified as key parameters affecting the hydrolysis rate.

In Eq. (**3.2**), the first term describes the formation of $S_2$ as a result of $S_1$ hydrolysis and the last two terms are expressed as double-Monod kinetics to represent the consumption of $S_2$ by $X_2$. Eq. (**3.3**) reproduces $S_3$ reduction to $S_4$, Eq. (**3.4**) describes the formation of $S_4$, which is further converted to $S_5$ according to Eq. (**3.5**). The two terms in Eq. (**3.6**) account for $S_6$ production via $S_3$ and $S_4$. Eqs. (**3.7**) and (**3.8**) describe the synthesis of new biomass as a result of substrate consumption and the decay of bacterial cells. Eq. (**3.7**) couples hydrolysis to the growth of $X_1$. Note that the Monod-type kinetics describing the bioconversion rates of $X_2$ in Eq. (**3.8**) include nitrite $S_3^*$ and nitrate $S_4^*$ threshold concentrations, which account for the inability of $X_2$ to grow below these values (Mattei et al., 2015b). The optimal values of $S_3^*$ and $S_4^*$ were estimated from the denitrification and denitritation experiments and were equal to 35 and 37 mg N/l, respectively. The ordinary differential equations (**3.1**) - (**3.8**) constituting the model were integrated by using an original code developed on the MATLAB platform based on the Runge-Kutta method. The comparison between the simulated results with the measured data was performed by evaluating the index of agreement (IoA) according to Esposito et al. (2011b).

# 3. RESULTS AND DISCUSSION

## 3.1 Kinetics of $S^0$-Based Denitrification and Denitritation

The evolution of the $NO_3^-$-N, $NO_2^-$-N and $SO_4^{2-}$-S concentration during the 3-week batch experiments is shown in **Figure 2**. Standard deviation values were below 5%. During

261 the $S^0$-driven autotrophic denitrification (**Figure 2A**), $NO_3^-$-N was first reduced to $NO_2^-$-N,
262 which was consequently converted into $N_2$. 62% of $NO_3^-$-N was transformed into $NO_2^-$-N.
263 The highest obtained removal rate for $NO_2^-$-N ($\nu_{NO2-N}$), which amounted to 8.0 mg $NO_2^-$-
264 N/l·d, was 2.6 times lower than that of $NO_3^-$-N ($\nu_{NO3-N}$) (**Table 3**). Nitrite accumulation
265 was most likely attributed to a higher activity of the $NO_3^-$-N reduction enzyme compared to
266 the $NO_2^-$-N reduction enzyme, as also reported elsewhere (Du et al., 2016; Sun and Nemati,
267 2012). The highest obtained $NO_3^-$-N removal rate of 20.9 mg $NO_3^-$-N/l·d was about 5 times
268 higher than that of a *Thiobacillus denitrificans* culture enriched on $S_2O_3^{2-}$ by Di Capua et al.
269 (2016).
270
271 **Table 3.** The highest $NO_3^-$-N and $NO_2^-$-N removal rates in $S^0$-driven autotrophic denitrification and
272 denitritation obtained using $S^0$ and biomass enriched on $NO_3^-$-N and $NO_2^-$-N.

| Experiment | $\nu_{NO3-N}$ [h] | $\nu_{NO2-N, ACCU}$ [i] | $\nu_{NO2-N}$ [j] | $\nu'_{NO2-N}$ [k] |
|---|---|---|---|---|
| Denitrification ($NO_3^-$ and $S^0$) [f] | 20.9 | 13.0 | 8.0 | - |
| Denitritation ($NO_2^-$ and $S^0$) [g] | - | - | - | 10.7 |
| Denitritation and denitrification ($NO_2^-$, $NO_3^-$ and $S^0$) [f] | 4.5 | - | 2.8 | 11.6 |

273 [f] Microbial source: biomass enriched for 3 months on $NO_3^-$-N and $S^0$
274 [g] Microbial source: biomass enriched for 3 months on $NO_2^-$-N and $S^0$
275 [h] $NO_3^-$-N reduction rate (mg $NO_3^-$-N/l·d)
276 [i] $NO_2^-$-N accumulation rate (mg $NO_2^-$-N/l·d)
277 [j] $NO_2^-$-N reduction rate in the presence of $NO_3^-$-N reduction (mg $NO_2^-$-N/l·d)
278 [k] $NO_2^-$-N reduction rate in the absence of $NO_3^-$-N reduction (mg $NO_2^-$-N/l·d)

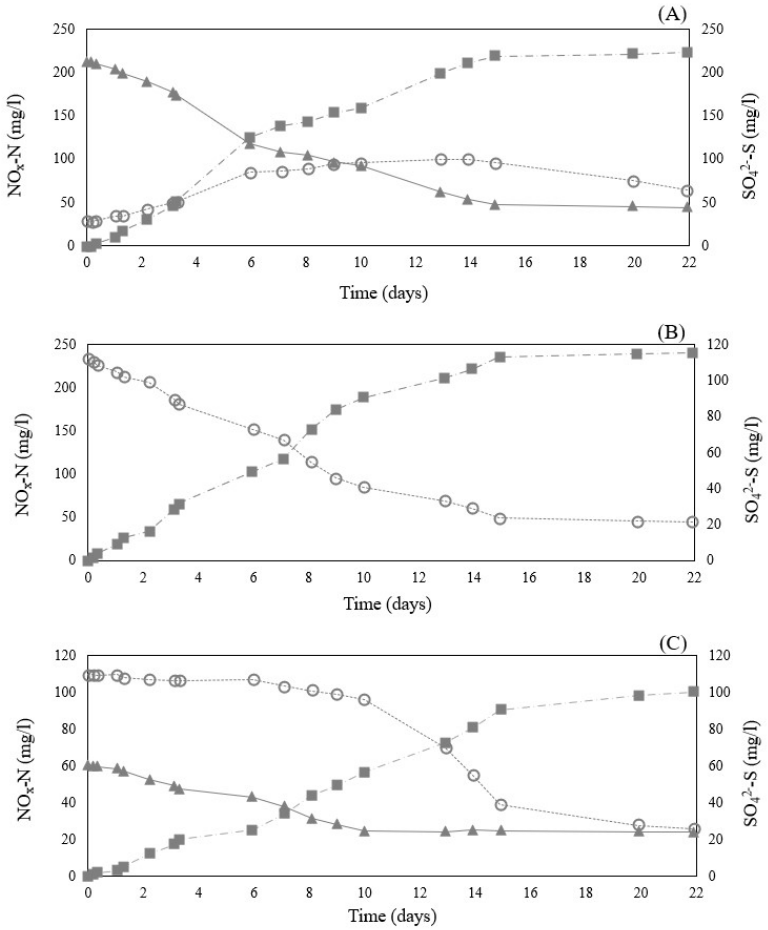


**Figure 2.** Kinetics of (A) denitrification, (B) denitritation, and (C) simultaneous denitritation and denitrification coupled to $S^0$ oxidation in batch experiments using $NO_3^-$-N, $NO_2^-$-N and $NO_3^-$-N with $NO_2^-$-N, respectively, as electron acceptors and $S^0$ as electron donor and biomass carrier at 30 (± 2)°C and pH of 7.4 (±0.2). $NO_3^-$-N (—▲—), $NO_2^-$-N (---○---) and $SO_4^{2-}$-S (– ■ –) concentrations profiles.

After 6 d of incubation in the kinetic tests, $NO_2^-$-N accumulated up to 85 mg/l and resulted in a drop of the $NO_3^-$-N removal rate to 7.0 mg/l·d. This might be attributed to the inhibition effect of $NO_2^-$-N on the activity of the denitrifying biomass. In other studies, the inhibition of denitrification has been observed at $NO_2^-$-N concentrations above 30 mg/l (Guerrero et al., 2016). The higher $NO_2^-$-N tolerance of the microbial consortia obtained in this study was likely due to an acclimation of 90 d, i.e. longer than the 60 d used by Di Capua et al. (2016).

After the first 2 weeks of experimentation, the $NO_3^-$-N removal efficiency reached up to 75%, resulting in a $NO_2^-$-N accumulation up to 100 mg/l. A higher $NO_2^-$-N accumulation is generally achieved when using $S^0$ as electron donor for autotrophic denitrification due to the low solubility of the $S^0$-based substrate (Campos et al., 2008; Sahinkaya et al., 2015; Simard et al., 2015; Soares, 2002). To increase the $S^0$ solubilization rate, $S^0$ particles with a higher specific surface area should be used, such as chemically synthesized $S^0$ powder (Di Capua et al., 2016). This both guarantees a better contact between the $S^0$ particles and the microorganisms and improves the $S^0$ dissolution kinetics (Sierra-Alvarez et al., 2007).

The denitritation kinetics were further studied in the presence of $NO_2^-$-N as the sole electron acceptor in order to investigate the potential of the biomass enriched on $NO_2^-$ to reduce high $NO_2^-$ concentrations (**Figure 2B**). The $NO_2^-$-N removal rate was 10.7 mg/l·d (**Figure 2B**), i.e. 1.3 times higher than that observed when $NO_3^-$-N and $NO_2^-$-N were concomitantly present, likely due to a longer acclimation of the biomass to $NO_2^-$ (**Figure 2B**). The denitrifying bacteria were capable of removing up to 81% of $NO_2^-$-N, similarly as observed by Sun and Nemati (2012). A $NO_2^-$-N concentration as high as 240 mg/l did not

have detrimental effects on denitritation. Therefore, the biomass enriched on $NO_2^-$ could be used to remove high $NO_2^-$ concentrations. For instance, the use of such acclimated biomass is recommended when $NO_2^-$ considerably accumulates during $S^0$-driven autotrophic denitrification treating high-strength $NO_3^-$ wastewaters.

In order to study the effect of high $NO_2^-$-N concentrations on denitrification, $NO_2^-$-N and $NO_3^-$-N were simultaneously fed in concentrations of 110 and 60 mg/l, respectively (**Figure 2C**). During the first 10 d, the $NO_3^-$-N removal efficiency was 67%. Simultaneously, $NO_2^-$-N removal occurred at a rate of 2.8 mg/l·d (**Table 3**). After 10 d, the $NO_2^-$-N removal rate increased up to 11.6 mg/l·d, demonstrating that the denitrifying bacteria initially preferred to use $NO_3^-$-N as electron acceptor compared to $NO_2^-$-N. Additionally, the presence of $NO_3^-$-N could inhibit the synthesis and activity of $NO_2^-$-N reductase (Philips et al., 2002). When $NO_3^-$-N removal stopped, denitrifying bacteria were still capable of removing $NO_2^-$-N (**Figure 2C**), as also reported elsewhere (Kilic et al., 2014; Sierra-Alvarez et al., 2007).

The maximum $NO_3^-$-N (20.9 mg/l·d) and $NO_2^-$-N (11.6 mg/l·d) removal rates coupled to $S^0$ oxidation were in the same order of magnitude of those obtained in other studies (Kilic et al., 2014; Sierra-Alvarez et al., 2007; Wang et al., 2016; Zhou et al., 2015). Because of the low $S^0$ water solubility and its bioavailability for microorganisms, the autotrophic denitrification and denitritation rates were lower compared to those obtained with other reduced soluble sulfur compounds such as $S_2O_3^{2-}$ (Mora et al., 2014; Zou et al., 2016). Therefore, the study of different sulfur sources with a higher bioavailability and a lower cost than chemically-synthesized $S^0$ lentils, such as biogenic $S^0$, might be of great interest for $S^0$-driven denitrification and denitritation applications.

The $SO_4^{2-}$-S concentration was in good agreement with the theoretical $SO_4^{2-}$-S production according to the stoichiometry (Sun and Nemati, 2012), except at the end of the denitrification experiment (**Figure 2**). In the abiotic and electron donor-free controls, denitrification and denitritation were not observed (data not shown).

### 3.2 Microbial Community Performing the $S^0$-Based Denitrification and Denitritation: Suspended Biomass versus Biofilm Attached onto the $S^0$ Lentils

SEM analysis showed a strong biomass colonization on the $S^0$ particles during both autotrophic denitrification and denitritation, demonstrating the potential of the $S^0$ particles as a biomass carrier (**Figure 3)**. The bacteria colonized the crevices of the $S^0$ particles likely providing a protection from shear stress (**Figure 3B)**. The close contact between the surface of the $S^0$ particles and the bacteria in the form of biofilm (**Figure 3C)** likely provided favorable conditions for the solubilization of $S^0$ to the intermediate soluble sulfur compounds, which were further oxidized to $SO_4^{2-}$. No biofilm formation was observed onto the $CaCO_3$ particles (**Figure 3A**).

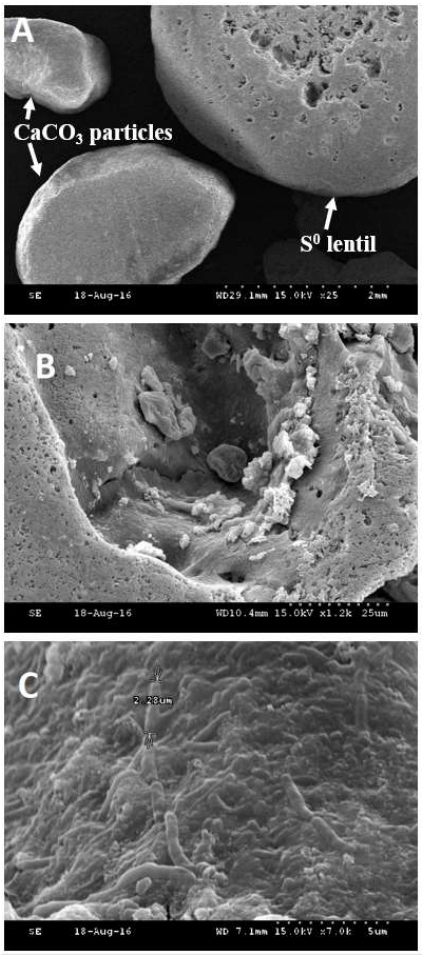


**Figure 3**. SEM image of (A) $S^0$ lentils (top right) and $CaCO_3$ particles (top left and bottom left) with a 25 times magnification; (B) the center of $S^0$ lentils with a $1.2 \cdot 10^3$ times magnification; (C) a $15 \cdot 10^3$ times magnification of the biofilm formed on the surface of $S^0$ lentils during the autotrophic denitrification and denitritation experiments.

352 **Figure 4** shows the bacterial diversity of the suspended biomass and biofilm
353 attached onto the $S^0$ lentils at the family level analyzed by the MiSeq. The raw activated
354 sludge collected from the municipal WWTP (Cassino, Italy) and used as inoculum
355 contained a microbial community with 4.2, 4.0, 3.6, 3.2 and 2.9% of *Comamonadaceae,*
356 *Saprospiraceae, Chitinophagaceae, Propionibacteriaceae* and rare families, respectively,
357 in addition to 58.2% of unclassified families. Other families were present at a relative
358 abundance below 2%. Despite the use of different electron acceptors, a similar community
359 structure was observed in the experiments performed with $NO_3^-$ and $NO_2^-$. This was also
360 observed by Zhou et al. (2011), who operated anaerobic up-flow biofilters with digested
361 sludge from a municipal WWTP as inoculum.
362 *Hydrogenophilaceae*, with a relative abundance below 0.1% in the inoculum, was
363 by far the largest family present in the kinetic experiments, both as suspended biomass and
364 biofilm attached onto the $S^0$ lentils with a relative abundance ranging between 36.7 and
365 59.9%. Most members of the *Hydrogenophilaceae* family are chemolithotrophic using
366 various inorganic electron donors such as reduced sulfur compounds (Rosenberg et al.,
367 2013). Previous research also demonstrated the predominance of *Hydrogenophilaceae* in
368 the community structure during $S^0$-oxidizing autotrophic denitrification (Zhang et al.,
369 2015a; Zhou et al., 2015) with *T. denitrificans* being the main species (Di Capua et al.,
370 2016; Kilic et al., 2014).

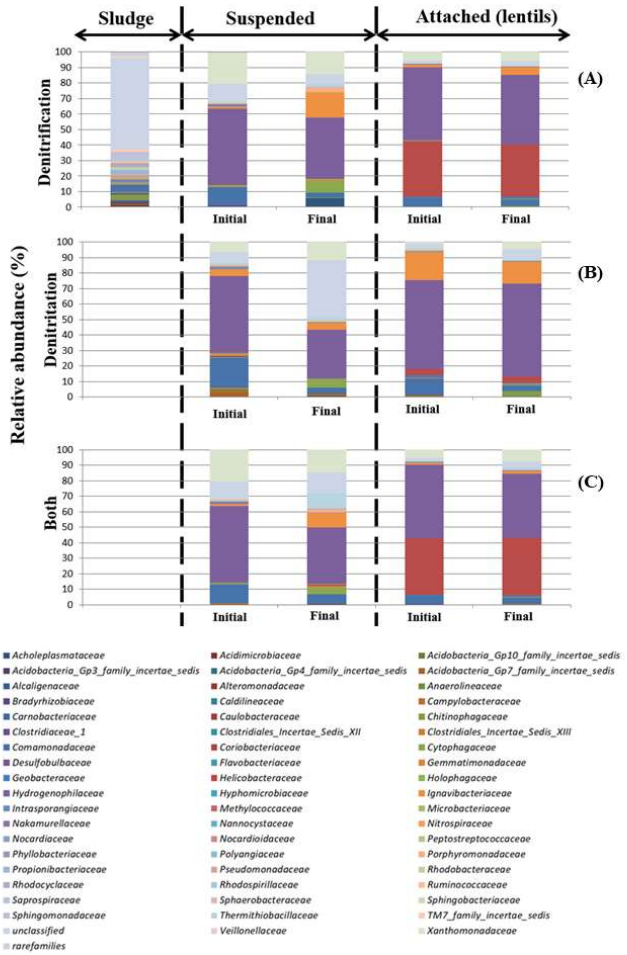


**Figure 4**. Relative abundance of bacterial families present in the raw activated sludge used as biomass source as well as microbial communities dominant in suspension and in the biofilm attached onto the $S^0$ lentils at the beginning (initial) and the end (final) of the autotrophic denitrification (A), autotrophic denitritation (B) and simultaneous autotrophic denitrification-denitritation (C) experiments.

In the suspended biomass, *Xanthomonadaceae*, *Comamonadaceae and Ignavibacteriaceae* were present with a relative abundance of 6.3-19.9%, 3.2-18.7% and 1.3-16.6%, respectively. Additionally, the families of *Xanthomonadaceae*, *Comamonadaceae* and *Ignavibacteriaceae* were also abundant in the biofilm attached onto the $S^0$ particles with a relative abundance of 1.1-7.6%, 3.5-10.1% and 1.5-18.2%, respectively. Microorganisms belonging to the *Xanthomonadaceae* family are capable of $NO_3^-$ and $NO_2^-$ respiration using organic products from cell lysis as electron donors (Xu et al., 2015), which would justify their presence in the denitrifying bioassays (**Figure 4**). *Comamonadaceae* is a large and diverse bacterial family that includes anaerobic denitrifiers and has been reported in previous $S^0$-based denitrification studies (Gao et al., 2017; Hao et al., 2017). *Ignavibacteriaceae* was recently identified as being associated with $S^0$-based autotrophic denitrifying processes (Zhang et al., 2015a, 2015b).

In this study, the dominating microbial community structure including the *Hydrogenophilaceae, Xanthomonadaceae*, *Comamonadaceae and Ignavibacteriaceae* families was similar for denitrification and denitritation experiments. Hence, the same bacterial families were likely capable to tolerate $NO_3^-N$ and $NO_2^-N$ concentrations up to 210 and 240 mg/l, respectively.

In the biofilm attached onto the $S^0$ particles, the distinct family of *Helicobacteraceae* was present with a relative abundance up to 37.1%. The high abundance of the bacteria belonging to this family in the biofilm (**Figures 4A and 4B**) was most likely associated with the $S^0$ hydrolysis (Boyd and Druschel, 2013), which is the necessary step prior to $S^0$-driven autotrophic denitrification or denitritation (Moraes and Foresti, 2012; Wang et al., 2016). Additionally, the presence of *Helicobacteraceae* was confirmed in the

simultaneous autotrophic denitrification-denitritation experiment (**Figure 4C**). Bacteria within the *Helicobacteraceae* family are known for their sulfur-oxidizing capacities in terrestrial and marine environments (Waite et al., 2017).

Families belonging to the sulfate-reducing bacteria (SRB), e.g. *Desulfobulbaceae*, in the activated sludge and kinetic experiments were observed with a relative abundance below 1%. Additionally, lower $SO_4^{2-}$ concentrations than those determined by the stoichiometry were observed at the end of the denitrification experiments, similarly as illustrated by Di Capua et al. (2016). This discrepancy might be attributed to the activity of these SRB using organics from bacterial lysis as electron donor. SRB likely played no role in the denitritation experiments as $NO_2^-$-N at concentrations higher than 170 mg/l are detrimental for their activity (Show et al., 2013).

### 3.3 Numerical Simulations of $S^0$-Based Two-Step Autotrophic Denitrification

Autotrophic denitrification and denitritation with $S^0$ are promising and efficient processes for the treatment of drinking water or $NO_3^-$ and $NO_2^-$ contaminated wastewater poor in organics (Liu et al., 2016; Zhang et al., 2015a; Zhou et al., 2015). The limitation of using $S^0$-based autotrophic denitrification and denitritation is associated with the low solubility of elemental $S^0$ (Park and Yoo, 2009; Wang et al., 2016), which decreases the rates of the entire process. Therefore, this work proposes a novel modeling interpretation of the $S^0$ solubilization step by hydrolytic microorganisms, prior to denitrification or denitritation.

In the mathematical model proposed in this study, the values of $\mu_{i,j}^{max}$ (**Table 2**) were lower compared to those obtained by Liu et al. (2016), most probably due to the

different microbial characteristics and enrichment procedure. The value of $\mu_{2,3}^{max}$ was slightly higher than $\mu_{2,4}^{max}$, resulting in a faster $NO_3^-$-N degradation than $NO_2^-$-N reduction and, thus, $NO_2^-$-N accumulation. Additionally, the similar values obtained for $\mu_{i,j}^{max}$ confirmed the presence of the same denitrifying bacterial biomass $X_2$ in the denitrification and denitritation experiments.

The dynamic simulations were compared with the experimental curves (**Figures 5** and **6**). Panels (A) and (B) of **Figure 5** refer to, respectively, $NO_3^-$-N removal during denitrification and $NO_2^-$-N removal in the denitritation experiments coupled to $SO_4^{2-}$-S production. **Figure 6** shows the system dynamics of $NO_3^-$-N reduction with $NO_2^-$-N as an intermediate product of denitrification (denitrification experiment).

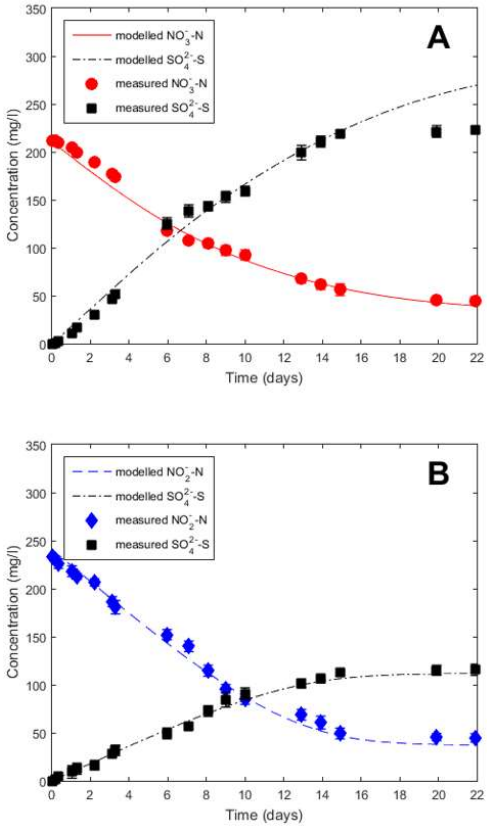


**Figure 5.** Experimental profiles and model predictions obtained for (A) the denitrification (initial condition: 210 mg/l of $NO_3^-$-N) and (B) denitritation (initial condition: 240 mg/l of $NO_2^-$-N) experiments using $S^0$ as an electron donor.

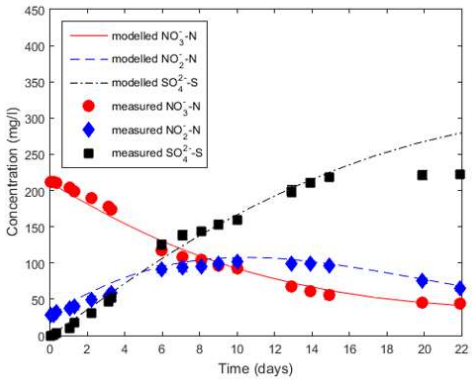


**Figure 6.** Experimental profiles and model predictions obtained for the two-step autotrophic denitrification experiment using $S^0$ as an electron donor. Initial conditions: 30 mg/l of $NO_2^-$-N and 210 mg/l of $NO_3^-$-N.

The model predictions matched reasonably well the measured data, except for the higher $SO_4^{2-}$-S production at the end of the experiments (**Figure 5A**). This was likely attributed to the development of a population of SRB in the presence of low amounts of organics from cell lysis, as SRB were present in the kinetic experiments (**Figure 4**). The influence of sulfate reduction on the mass balance of S-compounds during $S^0$-driven autotrophic denitrification needs further investigation. For this, the inclusion of the co-existence of denitrifiers and SRB in the model offers an elegant way to study these interactions. This was, however, out of the scope of the present study. A further extension of the model might be related to the explicit mathematical modelling of the biofilm growth onto the $S^0$ lentils by using a continuum approach (D'Acunto et al., 2017).

The consistency between the simulated and experimental results (**Figure 6**) demonstrated that the proposed model was able to account for $NO_3^-$ reduction, $NO_2^-$ accumulation, biomass growth, $S^0$ surface-based solubilization and oxidation during $S^0$-driven autotrophic denitrification. This was also confirmed by the high IoA values of 0.997, 0.985 and 0.990 obtained for $NO_3^-$-N, $NO_2^-$-N and $SO_4^{2-}$-S, respectively.

## 4. CONCLUSIONS

In the denitrification experiments with $S^0$, the highest $NO_3^-$-N removal rate of 20.9 mg/l·d was obtained. A $NO_2^-$-N removal rate of 10.7 mg/l·d was achieved even at a $NO_2^-$-N concentration of 240 mg/l, when the biomass enriched on $NO_2^-$ was used. The *Helicobacteraceae* family was only present in the biofilm attached onto the $S^0$ particles and was considered as the biomass capable of $S^0$ hydrolysis in the surface-based model. The two-step autotrophic denitrification kinetics were successfully simulated by the model as a sequential reduction of $NO_3^-$ to $NO_2^-$ and then to $N_2$ by denitrifying bacteria.

## ACKNOWLEDGMENTS

The authors gratefully thank the Cassino municipal wastewater treatment plant (Cassino, Italy) for providing the activated sludge. This work was supported by the Marie Skłodowska-Curie European Joint Doctorate (EJD) in Advanced Biological Waste-To-Energy Technologies (ABWET) funded by the Horizon 2020 program under the grant agreement no. 643071.

**Supplementary Material**

Supplementary data associated with this article can be found in the online version of the paper.

**Notes**

The authors have no competing interests to declare.

## REFERENCES


APHA, 2011. Standard Methods for the Examination of Water and Wastewater.

Barrett, M., Jahangir, M.M.R., Lee, C., Smith, C.J., Bhreathnach, N., Collins, G., Richards, K.G., O'Flaherty, V., 2013. Abundance of denitrification genes under different peizometer depths in four Irish agricultural groundwater sites. Environ. Sci. Pollut. Res. 20, 6646–6657. doi:10.1007/s11356-013-1729-3

Batchelor, B., Lawrence, A.W., 1978. A kinetic model for autotrophic denitrification using elemental sulfur. Water Res. 12, 1075–1084. doi:10.1016/0043-1354(78)90053-2

Boyd, E.S., Druschel, G.K., 2013. Involvement of intermediate sulfur species in biological reduction of elemental sulfur under acidic, hydrothermal conditions. Appl. Environ. Microbiol. 79, 2061–2068. doi:10.1128/AEM.03160-12

Campos, J.L., Carvalho, S., Portela, R., Mosquera-Corral, A., Méndez, R., 2008. Kinetics of denitrification using sulphur compounds: Effects of S/N ratio, endogenous and exogenous compounds. Bioresour. Technol. 99, 1293–1299. doi:10.1016/j.biortech.2007.02.007

Caporaso, J.G., Lauber, C.L., Walters, W.A., Berg-lyons, D., Lozupone, C.A., Turnbaugh,

P.J., Fierer, N., Knight, R., 2010. Global patterns of 16S rRNA diversity at a depth of millions of sequences per sample. Proc. Natl. Acad. Sci. U. S. A. 108, 4516–4522. doi:10.1073/pnas.1000080107/-/DCSupplemental.www.pnas.org/cgi/doi/10.1073/pnas.1000080107

Christianson, L., Lepine, C., Tsukuda, S., Saito, K., Summerfelt, S., 2015. Nitrate removal effectiveness of fluidized sulfur-based autotrophic denitrification biofilters for recirculating aquaculture systems. Aquac. Eng. 68, 10–18. doi:10.1016/j.aquaeng.2015.07.002

D'Acunto, B., Frunzo, L., Mattei, M.R., 2017. Continuum approach to mathematical modelling of multispecies biofilms. Ric. Mat. 66, 153–169. doi: 10.1007/s11587-016-0294-8.

Di Capua, F., Ahoranta, S.H., Papirio, S., Lens, P.N.L., Esposito, G., 2016. Impacts of sulfur source and temperature on sulfur-driven denitrification by pure and mixed cultures of *Thiobacillus*. Process Biochem. 51, 1576–1584. doi:10.1016/j.procbio.2016.06.010

Du, R., Peng, Y., Cao, S., Li, B., Wang, S., Niu, M., 2016. Mechanisms and microbial structure of partial denitrification with high nitrite accumulation. Appl. Microbiol. Biotechnol. 100, 2011–2021. doi:10.1007/s00253-015-7052-9

Esposito, G., Frunzo, L., Panico, A., Pirozzi, F., 2011a. Modelling the effect of the OLR and OFMSW particle size on the performances of an anaerobic co-digestion reactor. Process Biochem. 46, 557–565. doi:10.1016/j.procbio.2010.10.010

Esposito, G., Frunzo, L., Panico, A., Pirozzi, F., 2011b. Model calibration and validation for OFMSW and sewage sludge co-digestion reactors. Waste Manag. 31, 2527–2535.

522 doi:10.1016/j.wasman.2011.07.024
523 Gao, L., Zhou, W., Huang, J., He, S., Yan, Y., Zhu, W., Wu, S., Zhang, X., 2017. Nitrogen
524 removal by the enhanced floating treatment wetlands from the secondary effluent.
525 Bioresour. Technol. 234, 243–252. doi:10.1016/j.biortech.2017.03.036
526 Griffiths, R.I., Whiteley, A.S., Anthony, G., Donnell, O., Bailey, M.J., Donnell, A.G.O.,
527 2000. Rapid method for coextraction of DNA and RNA from natural environments for
528 analysis of ribosomal DNA- and rRNA-based microbial community composition.
529 Appl. Environ. Microbiol. 66, 5488–5491. doi:10.1128/AEM.66.12.5488-5491.2000
530 Guerrero, L., Montalvo, S., Huiliñir, C., Campos, J.L., Barahona, A., Borja, R., 2016.
531 Advances in the biological removal of sulphides from aqueous phase in anaerobic
532 processes: A review. Environ. Rev. 24, 84–100. doi:10.1139/er-2015-0046
533 Hao, R., Meng, C., Li, J., 2017. Impact of operating condition on the denitrifying bacterial
534 community structure in a 3DBER-SAD reactor. J. Ind. Microbiol. Biotechnol. 44, 9–
535 21. doi:10.1007/s10295-016-1853-4
536 Hills, D.J., Nakano, K., 1984. Effects of particle size on anaerobic digestion of tomato solid
537 wastes. Agric. Wastes 10, 285–295. doi:10.1016/0141-4607(84)90004-0
538 Kilic, A., Sahinkaya, E., Cinar, O., 2014. Kinetics of autotrophic denitrification process and
539 the impact of sulphur/limestone ratio on the process performance. Environ. Technol.
540 35, 2796–804. doi:10.1080/09593330.2014.922127
541 Li, W., Shan, X.Y., Wang, Z.Y., Lin, X.Y., Li, C.X., Cai, C.Y., Abbas, G., Zhang, M.,
542 Shen, L.D., Hu, Z.Q., Zhao, H.P., Zheng, P., 2016. Effect of self-alkalization on nitrite
543 accumulation in a high-rate denitrification system: Performance, microflora and
544 enzymatic activities. Water Res. 88, 758–765. doi:10.1016/j.watres.2015.11.003

Liu, Y., Peng, L., Ngo, H.H., Guo, W., Wang, D., Pan, Y., Sun, J., Ni, B.J., 2016. Evaluation of nitrous oxide emission from sulfide- and sulfur-based autotrophic denitrification processes. Environ. Sci. Technol. 50, 9407–9415. doi:10.1021/acs.est.6b02202

Mattei, M.R., Frunzo, L., D'Acunto, B., Esposito, G., Pirozzi, F., 2015a. Modelling microbial population dynamics in multispecies biofilms including Anammox bacteria. Ecol. Modell. 304, 44–58. doi:10.1016/j.ecolmodel.2015.02.007

Mattei, M.R., D'Acunto, B., Esposito, G., Frunzo, L., Pirozzi, F., 2015b. Mathematical modeling of competition and coexistence of sulfate-reducing bacteria, acetogens, and methanogens in multispecies biofilms. Desalin. Water Treat. 55, 740–748. doi:10.1080/19443994.2014.937764

Mora, M., López, L.R., Gamisans, X., Gabriel, D., 2014. Coupling respirometry and titrimetry for the characterization of the biological activity of a SO-NR consortium. Chem. Eng. J. 251, 111–115. doi:10.1016/j.cej.2014.04.024

Moraes, B.S., Foresti, E., 2012. Determination of the intrinsic kinetic parameters of sulfide-oxidizing autotrophic denitrification in differential reactors containing immobilized biomass. Bioresour. Technol. 104, 250–256. doi:10.1016/j.biortech.2011.11.050

Papirio, S., Ylinen, A., Zou, G., Peltola, M., Esposito, G., Puhakka, J. ~~a~~A, 2014. Fluidized-bed denitrification for mine waters. Part I: low pH and temperature operation. Biodegradation 25, 425–35. doi:10.1007/s10532-013-9671-0

Park, J.Y., Yoo, Y.J., 2009. Biological nitrate removal in industrial wastewater treatment: which electron donor we can choose. Appl Microbiol Biotechnol 82, 415–429. doi:10.1007/s00253-008-1799-1

Philips, S.; Laanbroek, H. J.; Verstraete, W., 2002. Origin, causus and effects of increased nitrite concentrations in aquatic environments. Rev. Environm Sci. Biotechnol 1, 115–141. doi:10.1023/A:1020892826575

Qambrani, N.A., Jung, Y.S., Yang, J.E., Ok, Y.S., Oh, S.-E., 2015. Application of half-order kinetics to sulfur-utilizing autotrophic denitrification for groundwater remediation. Environ. Earth Sci. 73, 3445–3450. doi:10.1007/s12665-014-3641-7

Rosenberg, E., Delong, E. F., Lory, S., Stackebrandt, E., and Thompson, F. (Ed.), 2013. *The prokaryotes: Alphaproteobacteria and Betaproteobacteria*. Springer, Berlin, Heidelberg. doi:10.1007/978-3-642-30197-1

Sahinkaya, E., Yurtsever, A., Aktaş, Ö., Ucar, D., Wang, Z., 2015. Sulfur-based autotrophic denitrification of drinking water using a membrane bioreactor. Chem. Eng. J. 268, 180–186. doi:10.1016/j.cej.2015.01.045

Schloss, P.D., Westcott, S.L., Ryabin, T., Hall, J.R., Hartmann, M., Hollister, E.B., Lesniewski, R.A., Oakley, B.B., Parks, D.H., Robinson, C.J., Sahl, J.W., Stres, B., Thallinger, G.G., Van Horn, D.J., Weber, C.F., 2009. Introducing mothur: Open-source, platform-independent, community-supported software for describing and comparing microbial communities. Appl. Environ. Microbiol. 75, 7537–7541. doi:10.1128/AEM.01541-09

Show, K.Y., Lee, D.J., Pan, X., 2013. Simultaneous biological removal of nitrogen-sulfur-carbon: Recent advances and challenges. Biotechnol. Adv. 31, 409–420. doi:10.1016/j.biotechadv.2012.12.006

Sierra-Alvarez, R., Beristain-Cardoso, R., Salazar, M., Gómez, J., Razo-Flores, E., Field, J.A., 2007. Chemolithotrophic denitrification with elemental sulfur for groundwater

treatment. Water Res. 41, 1253–1262. doi:10.1016/j.watres.2006.12.039

Simard, M.-C., Masson, S., Mercier, G., Benmoussa, H., Blais, J.-F., Coudert, L., 2015. Autotrophic denitrification using elemental sulfur to remove nitrate from saline aquarium waters. J. Environ. Eng. 141, 4015037. doi:10.1061/(ASCE)EE.1943-7870.0000977

Sin, G., Kaelin, D., Kampschreur, M.J., Takács, I., Wett, B., Gernaey, K. V, Rieger, L., Siegrist, H., Van Loosdrecht, M.C.M., 2008. Modelling nitrite in wastewater treatment systems: A discussion of different modelling concepts. Water Sci. Technol. 58, 1155–1171. doi:10.2166/wst.2008.485

Soares, M.I.M., 2002. Denitrification of groundwater with elemental sulfur. Water Res. 36, 1392–1395. doi:10.1016/S0043-1354(01)00326-8

Sun, Y., Nemati, M., 2012. Evaluation of sulfur-based autotrophic denitrification and denitritation for biological removal of nitrate and nitrite from contaminated waters. Bioresour. Technol. 114, 207–216. doi:10.1016/j.biortech.2012.03.061

Vavilin, V.A., Fernandez, B., Palatsi, J., Flotats, X., 2008. Hydrolysis kinetics in anaerobic degradation of particulate organic material: An overview. Waste Manag. 28, 939–951. doi:10.1016/j.wasman.2007.03.028

Waite, D.W., Vanwonterghem, I., Rinke, C., Parks, D.H., Zhang, Y., Takai, K., Sievert, S.M., Simon, J., Campbell, B.J., Hanson, T.E., Woyke, T., Klotz, M.G., Hugenholtz, P., 2017. Comparative genomic analysis of the class *Epsilonproteobacteria* and proposed reclassification to epsilonbacteraeota (phyl. nov.). Front. Microbiol. 8. doi:10.3389/fmicb.2017.00682

Wang, Y., Bott, C., Nerenberg, R., 2016. Sulfur-based denitrification: Effect of biofilm

development on denitrification fluxes. Water Res. 100, 184–193. doi:10.1016/j.watres.2016.05.020

Xu, G., Peng, J., Feng, C., Fang, F., Chen, S., Xu, Y., Wang, X., 2015. Evaluation of simultaneous autotrophic and heterotrophic denitrification processes and bacterial community structure analysis. Appl. Microbiol. Biotechnol. 99, 6527–6536. doi:10.1007/s00253-015-6532-2

Xu, G., Yin, F., Chen, P.S., Xu, Y., Yu, P.H., 2016. Mathematical modeling of autotrophic denitrification (AD) process with sulphide as electron donor. Water Res. 91, 225–234. doi:10.1016/j.watres.2016.01.011

Zhang, L., Zhang, C., Hu, C., Liu, H., Bai, Y., Qu, J., 2015a. Sulfur-based mixotrophic denitrification corresponding to different electron donors and microbial profiling in anoxic fluidized-bed membrane bioreactors. Water Res. 85, 422–431. doi:10.1016/j.watres.2015.08.055

Zhang, L., Zhang, C., Hu, C., Liu, H., Qu, J., 2015b. Denitrification of groundwater using a sulfur-oxidizing autotrophic denitrifying anaerobic fluidized-bed MBR: performance and bacterial community structure. Appl. Microbiol. Biotechnol. 99, 2815–2827. doi:10.1007/s00253-014-6113-9

Zhou, W., Liu, X., Dong, X., Wang, Z., Yuan, Y., Wang, H., He, S., 2015. Sulfur-based autotrophic denitrification from the micro-polluted water. J. Environ. Sci. (China) 44, 180–188. doi:10.1016/j.jes.2016.01.002

Zhou, W., Sun, Y., Wu, B., Zhang, Y., Huang, M., Miyanaga, T., Zhang, Z., 2011. Autotrophic denitrification for nitrate and nitrite removal using sulfur-limestone. J. Environ. Sci. 23, 1761–1769. doi:10.1016/S1001-0742(10)60635-3

Zou, G., Papirio, S., van Hullebusch, E.D., Puhakka, J.A., 2015. Fluidized-bed denitrification of mining water tolerates high nickel concentrations. Bioresour. Technol. 179, 284-290. doi:10-1016/j.biortech.2014.12.044

Zou, G., Papirio, S., Lakaniemi, A.-M., Ahoranta, S.H., Puhakka, J.A., 2016. High rate autotrophic denitrification in fluidized-bed biofilm reactors. Chem. Eng. J. 284, 1287–1294. doi:10.1016/j.cej.2015.09.074